Published in final edited form as:
J Membr Biol. 2012 June ; 245(5-6): 221–230. doi:10.1007/s00232-012-9443-5.

Cytoplasmic Amino Acids within the Membrane Interface Region Influence Connexin Oligomerization

Tekla D. Smith,
Division of Pulmonary, Allergy, and Critical Care Medicine, Department of Medicine, Emory University School of Medicine, Whitehead Biomedical Research Building, 615 Michael St., Suite 205, Atlanta, GA 30022, USA

Aditi Mohankumar,
Department of Pediatrics, Section of Hematology/Oncology, University of Chicago, Chicago, IL 60637, USA

Peter J. Minogue,
Department of Pediatrics, Section of Hematology/Oncology, University of Chicago, Chicago, IL 60637, USA

Eric C. Beyer,
Department of Pediatrics, Section of Hematology/Oncology, University of Chicago, Chicago, IL 60637, USA

Viviana M. Berthoud, and
Department of Pediatrics, Section of Hematology/Oncology, University of Chicago, Chicago, IL 60637, USA

Michael Koval
Division of Pulmonary, Allergy, and Critical Care Medicine, Department of Medicine, Emory University School of Medicine, Whitehead Biomedical Research Building, 615 Michael St., Suite 205, Atlanta, GA 30022, USA

Department of Cell Biology, Emory University School of Medicine, Atlanta, GA 30322, USA

Michael Koval: mhkoval@emory.edu

Abstract

Gap junction channels composed of connexins connect cells, allowing intercellular communication. Their cellular assembly involves a unique quality-control pathway. Some connexins [including connexin43 (Cx43) and Cx46] oligomerize in the *trans*-Golgi network following export of stabilized monomers from the endoplasmic reticulum (ER). In contrast, other connexins (e.g., Cx32) oligomerize early in the secretory pathway. Amino acids near the cytoplasmic aspect of the third transmembrane domain have previously been shown to determine this difference in assembly sites. Here, we characterized the oligomerization of two connexins expressed prominently in the vasculature, Cx37 and Cx40, using constructs containing a C-terminal dilysine-based ER retention/retrieval signal (HKKSL) or treatment with brefeldin A to block ER vesicle trafficking. Both methods led to intracellular retention of connexins, since the cells lacked gap junction plaques. Retention of Cx40 in the ER prevented it from oligomerizing, comparable to Cx43. By contrast, ER-retained Cx37 was partially oligomerized. Replacement of

Correspondence to: Michael Koval, mhkoval@emory.edu.

Electronic supplementary material The online version of this article (doi:10.1007/s00232-012-9443-5) contains supplementary material, which is available to authorized users.

two amino acids near the third transmembrane domain of Cx43 (L152 and R153) with the corresponding amino acids from Cx37 (M152 and G153) resulted in early oligomerization in the ER. Thus, residues that allow Cx37 to oligomerize early in the secretory pathway could restrict its interactions with coexpressed Cx40 or Cx43 by favoring homomeric oligomerization, providing a structural basis for cells to produce gap junction channels with different connexin composition.

Keywords

Endothelium; Membrane traffic; Quality control; Chaperone; ERp29

Introduction

Cell–cell contact sites known as “gap junctions” facilitate intercellular communication by enabling the direct transfer of small metabolites and ions between adjacent cells. Gap junctions consist of arrays of channels formed by proteins in the connexin (Cx) family (Beyer and Berthoud 2009). A complete gap junction channel is formed by two hexameric hemichannels, one in each cell, that are transported to the plasma membrane, where they dock to form a complete intercellular channel (Laird 2006) and then assemble into semicrystaline arrays known as “gap junction plaques” (Johnson et al. 1974, 2012).

Oligomerization of connexin hemichannels is regulated by a unique quality-control pathway, which is still being elucidated (Koval 2006; Laird 2010). Different connexins show substantial differences in oligomerization. One connexin, Cx43, is stabilized in the endoplasmic reticulum (ER) by a chaperone protein, ERp29, that enables it to be transported as a monomer through the secretory pathway to the *trans*-Golgi apparatus, where it oligomerizes into hexameric hemichannels (Das et al. 2009; Musil and Goodenough 1993). In contrast, Cx32 does not interact with ERp29 and oligomerizes in the ER (Das et al. 2009). The quality control of Cx43 depends upon the amino acids flanking the third transmembrane (TM3) domain. Specifically, substituting tryptophan for arginine at amino acid position 153 in the cytosolic aspect of TM3 destabilizes monomeric Cx43 and causes its early oligomerization in the ER (Maza et al. 2003, 2005). Moreover, two dominant Cx43 mutations adjacent to R153 (T154A and T154N) are associated with oculodentodigital dysplasia (ODDD), underscoring the importance of this motif in the proper function of Cx43 (Paznekas et al. 2009).

Analysis of the cytoplasmic aspect of TM3 in the members of the connexin family reveals conserved motifs among subgroups of connexins that may determine cellular sites of oligomerization (Fig. 1). These connexin motifs fall into three subcategories: R-type, such as Cx43; W-type, including Cx32; and a third group that does not have clear homology with either the R- or W-type connexins (Table 1). Based on previous analysis of Cx43 and Cx32 (Maza et al. 2005), connexins in the R group are predicted to be highly stabilized as monomers in the ER, whereas connexins in the W group would oligomerize early within the secretory pathway. However, it is difficult to predict a priori whether connexins containing a cytoplasmic membrane interface region of TM3 that does not conform to either the R or the W motif would behave more like Cx43 or Cx32 in the ER.

We sought to determine the oligomerization properties of two connexins, Cx37 and Cx40, that do not contain either an R or a W motif. Cx37 and Cx40 are among the four major connexins expressed throughout the vasculature (Cx37, Cx40, Cx43 and Cx45) (Johnstone et al. 2009; Brisset et al. 2009). Connexin expression in the major cell types of blood vessels, endothelial cells and smooth muscle cells, is heterogeneous. Moreover, connexin composition of different classes of vascular gap junctions varies depending upon the

vascular bed examined (Severs et al. 2001). For example, myoendothelial junctions of mesentery and cremaster microvessels both contain abundant Cx40 and low levels of Cx45 but differ dramatically in Cx37 and Cx43 content (Isakson et al. 2008; Heberlein et al. 2009). Thus, endothelial cells differentially process and sort connexins between myoendothelial junctions and endothelial–endothelial cell junctions. Since Cx37, Cx40 and Cx45 are all compatible to formmixed (heteromeric) connexons with Cx43 (Beyer et al. 2001), the ability to alter myoendothelial connexin content requires that endothelial cells regulate oligomerization.

Since Cx37 and Cx40 have TM3 interface regions that do not fit well into either the R or W subcategories (Table 1) (Figueroa et al. 2004), we could not predict how their oligomerization would be regulated. In the current study, we assessed the oligomerization state of Cx37 and Cx40 in the ER and found that they differed in monomer stability and in the subcellular compartments where oligomerization occurs. These connexin-specific differences likely affect connexin targeting and hetero-oligomerization.

Methods

Antibodies and Reagents

Polyclonal rabbit anti-Cx37 antibodies were generated against a maltose binding protein-Cx37 fusion protein containing amino acids 80–333 of human Cx37. Anti-PDIA1 (PDI), -GM130 and -Cx43 antibodies were from Sigma (St. Louis, MO). Anti-Cx40 antibodies and monoclonal anti-Cx43 antibody were obtained from Chemicon (Temecula, CA). Fluorescent and horseradish peroxidase (HRP)-conjugated secondary antibodies were from Jackson ImmunoResearch (West Grove, PA). Triton X-100 was from Roche Molecular Biochemicals (Indianapolis, IN). Unless otherwise specified, all other reagents were from Sigma.

Generation of Connexin Constructs

Wild-type and HKKSL-containing Cx37 and Cx40 constructs were generated by PCR using human Cx37 in pSFFV-neo (Reed et al. 1993) or human Cx40 in pBScript (Kanter et al. 1994) as templates, the corresponding primers (Supplementary Table 1) and LA Taq DNA polymerase (Takara Mirus Bio, Madison, WI) or Phusion DNA polymerase (New England BioLabs, Ipswitch, MA). Primers were designed to incorporate *Hin*dIII and *Bam*HI restriction sites flanking the coding region. In the case of the HKKSL-containing constructs, primers were designed to incorporate the ER-retention signal HKKSL appended to the carboxyl terminus of the connexin. PCR products were subcloned in pGEM-T Easy (Promega, Madison, WI) or pCR4Blunt-TOPO vector (Life Technologies, Grand Island, NY); then, the *Bam*HI–*Hin*dIII inserts from these plasmids were subcloned into the corresponding sites of pcDNA3.1/Hygro (+) (Invitrogen).

To obtain the HKKSL-containing Cx43 mutants, primers facing opposite directions and spanning the DNA region encoding the mutated amino acids were designed to amplify the sequence of the full construct (Cx43-HKKSL including the vector sequence) according to the strategy used previously (Minogue et al. 2005); the plasmid was regenerated by religation of the PCR product. Cx43R153G and Cx43L152MR153G without the ER-retention signal were obtained by PCR using the HKKSL-containing constructs as templates and the primers listed in Supplementary Table 1; PCR products were subcloned in pCR-Blunt II-TOPO vector. The *Bam*HI–*Xho*I inserts of all Cx43 mutants were subcloned into the *Bam*HI-*Xho*I sites of pcDNA3.1/Hygro (+) vector.

The coding region of all constructs was fully sequenced at the Cancer Research Center DNA Sequencing Facility of the University of Chicago to ensure that PCR amplification did not introduce additional unwanted mutations.

Cell Culture

HeLa cells transfected with connexin constructs were prepared as previously described (Daugherty et al. 2007; Maza et al. 2003) and cultured in minimum essential medium containing Earle's salts, L-glutamine, 10 % heat-inactivated bovine calf serum, 100 IU/ml penicillin, 100 μg/ml streptomycin and 0.5 mg/ml Geneticin (Invitrogen) or 132 μg/ml hygromycin (EMD Millipore, Billerica, MA).

Immunofluorescence

For immunofluorescence, cells cultured on glass coverslips were fixed and permeabilized with methanol/acetone (1:1), then washed three times with PBS, followed by PBS + 0.5 % Triton X-100 and PBS + 0.5 % Triton X-100 + 2 % goat serum (PBS/GS). Cells were incubated with primary antibodies diluted into PBS/GS for 1 h, rinsed and then labeled with secondary antibodies diluted into PBS/GS. Cells were then rinsed with PBS, and coverslips were mounted on microscope slides with MOWIOL (Polysciences, Warren, PA). Images of the fluorescence signal were obtained using an Olympus (Tokyo, Japan) IX-70 microscope system with a Hamamatsu (Shizuoka, Japan) Orca-1 CCD camera and Image-Pro image analysis software (Media Cybernetics, Silver Spring, MD).

Sucrose Gradient Fractionation

Postnuclear homogenates were prepared with a ball-bearing homogenizer and centrifugation as previously described (Koval et al. 1995, 1997; Das Sarma et al. 2002). Postnuclear homogenates were solubilized in 1 % Triton X-100 for 30 min at 4 °C as described (Maza et al. 2005). Samples were then centrifuged at 100,000×*g* for 30 min, and the resulting Triton X-100-soluble fraction was overlaid onto a 5–18 % sucrose gradient on a 25 % sucrose cushion. Gradients were centrifuged at 148,000×*g* for 16 h at 4 °C in a Sorvall Ultra Pro 80 centrifuge (Thermo Scientific, Asheville, NC) using an AH-650 swinging bucket rotor. Following centrifugation, 0.2-ml fractions were collected from the bottom of the gradient at 4 °C. Samples were added to 2× sample buffer containing 50 mM DTT, resolved by SDS-PAGE, transferred to Immobilon P membranes and blotted. Specific signals corresponding to a given protein were detected by immunoblot using enhanced chemiluminescence (ECL) reagent (GE Healthcare, Piscataway, NJ) and quantified with a BioRad Image Lab system (Hercules, CA). The extent of oligomerization was calculated as the percentage of the total area under the curve from the sucrose gradient curves corresponding to the hexamer peak. Statistical significance was assessed by Student's *t* test.

Blue Native Gel Electrophoresis

Nondenaturing, blue native gel electrophoresis was done using a method based on that of Wittig et al. (2006). Cells were either untreated or treated for 5 h with 6 μg/ml brefeldin A. Cells were homogenized and postnuclear supernatants were diluted into BN Sample Buffer [50 mg/ml Serva G (coomassie blue, G250), 30 % glycerol in ddH_2O]. Blue native gels consisted of a 4.2 % polyacrylamide stacking gel on a 7.5 % resolving gel in Bis Tris–HCl, pH 7.0. Five microliters of each sample were loaded per lane, and the gels were run using 50 mM Tricine/15 mM Bis Tris (pH 7.0) cathode buffer containing 0.01 % Serva G and 50 mM Bis Tris–HCl on ice. Gels were run at constant voltage (100 V) on ice for 3–6 h until the blue dye migrated approximately two-thirds of the way along the resolving gel. The cathode buffer was replaced with a dyefree cathode buffer and the gel run to completion at 150 V constant voltage for 2 h. Gels were removed and incubated in transfer buffer (50 mM Tris,

380 mM glycine, 0.025 % SDS, 20 % MeOH) for 30 min at room temperature, and proteins were transferred to Immobilon P using a BioRad semidry apparatus. Blots were processed using a standard immunoblot protocol, using appropriate primary antibodies, HRP-conjugated goat anti-rabbit IgG secondary antibodies and ECL for detection. Lanes were scanned and analyzed using Image-Pro software.

Results

To examine the cellular sites of oligomerization of Cx40 and Cx37, we applied an approach previously used to study early events in Cx43 and Cx32 oligomerization by producing connexin constructs tagged with a C-terminal HKKSL ER-retention/retrieval motif, Cx40-HKKSL and Cx37-HKKSL (Das Sarma et al. 2002, 2005, 2008; Maza et al. 2003, 2005). Using transfected HeLa cells, we found that wild-type (untagged) Cx40 was transported to the plasma membrane, where it formed gap junction plaques. However, Cx40-HKKSL was retained in the ER (Fig. 2). Sucrose gradient fractionation revealed that the sedimentation profile of Cx40-HKKSL was indistinguishable from that of Cx43-HKKSL (Fig. 2). Thus, Cx40-HKKSL is retained in the ER as stabilized monomers, suggesting that the itinerary of Cx40 oligomerization is comparable to that of Cx43.

We performed a similar analysis of Cx37 and Cx37-HKKSL. As expected, untagged Cx37 was transported to the plasma membrane, while Cx37-HKKSL was retained in the ER (Fig. 3). To further confirm that Cx37-HKKSL was predominantly localized to the ER, immunofluorescence colocalization was performed using markers for the ER (PDI) and *cis*-Golgi apparatus (GM130). Cx37-HKKSL predominantly colocalized with PDI, consistent with ER retention (Fig. 4). There was also some colocalization with GM130; however, this appeared to be a relatively minor intracellular component of Cx37-HKKSL.

In contrast to Cx40-HKKSL and Cx43-HKKSL, the sucrose gradient fractionation profile of Cx37-HKKSL had a more complex pattern. One peak sedimented at the same percentage of sucrose (10 %) as the predominant peak of untagged Cx37 representing oligomerized Cx37 (Fig. 3). These results suggest that Cx37-HKKSL retained in the ER was partially oligomerized.

As an independent method to examine the oligomerization state of Cx37 retained in the ER, we examined HeLa cells transfected with untagged Cx37 by blue native gel electrophoresis (Fig. 5). In control HeLa/Cx37 cells, Cx37 exhibited comparable hexamer and monomer peaks. Importantly, when these cells were treated with brefeldin A for 5 h to inhibit membrane efflux from the ER, Cx37 oligomerization was not affected. In contrast, this treatment significantly inhibited Cx43 oligomerization (Fig. 5).

The cytoplasmic interface region of TM3 is necessary to stabilize monomeric Cx43 in the ER (Maza et al. 2005). Since Cx37 has a distinct motif in this region, we examined whether changing the Cx43 LR motif to the MG motif found in Cx37 would affect the extent of Cx43 oligomerization in the ER. As shown in Fig. 6, this was indeed the case for the two mutant Cx43 constructs, Cx43R153G-HKKSL and Cx43L152MR153G-HKKSL. In fact, the sedimentation profile and amount of ER oligomerized protein were equivalent for Cx43L152MR153G-HKKSL and Cx37-HKKSL. As a control for misfolding induced by these point mutations, we examined the ability of untagged Cx43R153G and Cx43L152MR153G to form gap junction plaques (Fig. 7). Both of these proteins were transported to the plasma membrane, where they assembled into gap junction plaques, suggesting that the proteins were properly processed. Taken together, these data suggest that the MG motif plays an important role in promoting early oligomerization of Cx37.

Discussion

We found that Cx37, unlike Cx43, has the capacity to oligomerize in the ER. We could mimic this behavior by mutating two key amino acid residues of Cx43 in the cytoplasmic interface region of TM3 to the corresponding amino acids of Cx37. This observation extends previous studies demonstrating that R153 was required to stabilize monomeric Cx43 in the ER (Maza et al. 2005). In the present study, we consistently observed an increase in ER oligomerization of Cx43 when both L152 and R153 were mutated to MG. Moreover, mutation of only R153 to glycine in Cx43-HKKSL resulted in variable ER oligomerization compared with Cx40 or Cx43. However, the cytoplasmic arginine residue is not an absolute requirement to stabilize connexin monomers in the ER since Cx40-HKKSL was retained as monomers in the ER, despite the presence of an asparagine at the corresponding position in this connexin. Thus, the amino group of the carboxamide in the N151 side chain of Cx40 can substitute for the function of a guanidinium amino group in R153 of Cx43.

By sequence analysis, we defined three classes of motifs in the plasma membrane–cytoplasm interface of TM3. Several connexins have a conserved, positively charged arginine or lysine residue in this region of TM3 (Table 1), which we have designated as the R motif. Based on the behavior of Cx43, we anticipate that other R-motif connexins are highly stabilized as monomers in the ER and subsequently oligomerized in the *trans*-Golgi network (Maza et al. 2005). Consistent with this hypothesis, Cx46, which contains an R-motif sequence identical to that of Cx43 (LLRTY), oligomerizes in the Golgi apparatus (Koval et al. 1997). We anticipate that the other R-type connexins will also remain monomeric in the ER, due to the presence of the conserved arginine/lysine residue; however, the stability of connexins containing R-type motifs that are not identical to Cx43 could be influenced by surrounding amino acids as well.

Our results imply that Cx43 domains on both sides of the ER membrane are critical for regulating monomer stability and oligomerization. Stabilization of monomeric Cx43 in the ER requires an interaction of ERp29 (a luminal chaperone) with the second extracellular loop domain of Cx43 (Das et al. 2009). Our current and previous results also emphasize the importance of L152 and R153 at the cytoplasmic side of TM3 in regulating oligomerization. These results suggest a sequence of events in which the dissociation of ERp29 from monomeric Cx43 leads to conformational changes involving TM3 that alter the exposure of L152 and R153, which in turn allows oligomerization with other Cx43 monomers.

We anticipate that ERp29 will interact with other connexins as well. Interestingly, development of cataracts in Cx46-deficient mice is sensitive to strain background; cataracts are more severe in lenses of mice that are deficient in ERp29 (129/SvJ) than in lenses of mice with high levels of ERp29 (C57Bl6) (Gong et al. 1999; Hoehenwarter et al. 2008). This difference may be explained by a role for ERp29 in regulating oligomerization and trafficking of the second connexin (Cx50, which has an LLRTY motif) that is also expressed in lens fiber cells and may partially compensate for the loss of Cx46. Whether other R-type connexins can bind to ERp29 remains to be determined. It is likely that interactions between connexins and ERp29 will be influenced by the identity of amino acids in the extracellular loop domains in addition to those in the membrane interface regions of the TM3 domain.

In contrast with Cx43, Cx32, which has a WW motif instead of the LR motif, oligomerizes in the ER. By analogy, this suggests that other W-type connexins may also oligomerize in the ER. We propose that the presence of a highly charged arginine (rather than a bulky hydrophobic residue) at the TM3–membrane interface in R-type connexins determines their subcellular site of oligomerization by allowing TM3 the conformational flexibility needed to stabilize monomers in the ER membrane and, thus, restrict oligomerization until they reach

the *trans*-Golgi. Moreover, the lack of a highly charged residue in the "MG" motif of Cx37 is likely to have a destabilizing effect since introduction of this motif into Cx43 destabilized it in the ER as well. In addition, the finding that Cx40 and Cx43 remain monomeric in the ER suggests that in order to completely block ER oligomerization, the side chain of the amino acid corresponding to R153 in Cx43 at the TM3–membrane interface may require an amino group (R, K or N). Distinguishing between these possibilities will require structural models for monomeric Cx43 and further experimentation.

Cells expressing multiple connexin genes have the potential to form heteromeric hexamers in addition to homomeric hexamers. Hetero-oligomerization is a regulated process, and connexins must be compatible to interact in order to form a heteromeric hemichannel (Cottrell and Burt 2005; Koval 2006). For instance, Cx26 and Cx43 are incompatible to hetero-oligomerize; however, replacing the TM3 domain of Cx26 with amino acids 154–174 from the TM3 domain of Cx43 creates a chimera that can heterooligomerize with both Cx26 and Cx43 (Martinez et al. 2011). While the dual compatibility for this chimera indicates an important role for TM3 in defining connexin compatibility, it also suggests that other residues contribute to the control of connexin oligomerization. Consistent with this, N-terminal variants of Cx43 (e.g., D12S, K13G) interact with Cx32 (Lagree et al. 2003). However, these mutations did not support hetero-oligomerization with Cx26, indicating that other, as yet to be determined structural motifs promote an interaction with Cx26 (Gemel et al. 2004). However, mechanisms that favor homo-oligomerization are also important. For instance, the C-terminal domain of Cx43 dimerizes as well as interacts with the cytoplasmic loop domain in a pH-dependent manner (Hirst-Jensen et al. 2007).

Although Cx37, Cx40 and Cx43 can hetero-oligomerize, incorporation of these three connexins into gap junctions in the vascular bed is regulated. Using a coculture model where cells maintained polarity and phenotype, Isakson and Duling (2005) found that Cx37 was specifically excluded from myoendothelial junctions between aortic endothelial cells and vascular smooth muscle cells. Instead, Cx37 was incorporated into junctions interconnecting either two adjacent endothelial cells or two adjacent smooth muscle cells. Immunohistochemical analysis is consistent with this result since there is partial colocalization between Cx37 and Cx40 or Cx43 in situ (Gabriels and Paul 1998; Severs et al. 2001). Triple heteromers consisting of Cx37, Cx40 and Cx43 have not been biochemically isolated, although there is immunohistochemical evidence showing all three connexins in the same endothelial gap junction plaque (Yeh et al. 1998). We speculate that differences in subcellular sites of oligomerization between Cx37, Cx40 and Cx43 and in their ability to interact with the connexin quality-control pathway play key roles in determining connexin sorting to different plasma membrane domains. Given that Cx40 and Cx43 oligomerization are comparably regulated, there is likely to be a prevalence of Cx40/Cx43 hetero-oligomers over those containing Cx37. In particular, since different types of microvessels exhibit differences in myoendothelial junction composition (Isakson et al. 2008), cells require the ability to regulate connexin homo- and hetero-oligomerization. Identifying elements of the connexin quality-control pathway that differentially control connexin oligomerization and trafficking will help to define the cellular mechanisms used to regulate gap junction composition.

Supplementary Material

Refer to Web version on PubMed Central for supplementary material.

Acknowledgments

This work was supported by the Emory Alcohol and Lung Biology Center/National Institutes of Health grants P50-AA013757 (M. K.), R01-HL083120 (M. K.), RO1-HL59199 (E. C. B.) and RO1-EY08368 (E. C. B.) and by the Emory University Research Committee (M. K.).

References

Beyer, EC.; Berthoud, VM. The family of connexin genes. In: Harris, AL.; Locke, D., editors. Connexins: a guide. New York: Humana Press; 2009. p. 3-26.

Beyer EC, Gemel J, Martinez A, Berthoud VM, Valiunas V, Moreno AP, Brink PR. Heteromeric mixing of connexins: compatibility of partners and functional consequences. Cell Commun Adhes. 2001; 8:199–204. [PubMed: 12064588]

Brisset AC, Isakson BE, Kwak BR. Connexins in vascular physiology and pathology. Antioxid Redox Signal. 2009; 11:267–282. [PubMed: 18834327]

Chen J, Anderson JB, DeWeese-Scott C, Fedorova ND, Geer LY, He S, Hurwitz DI, Jackson JD, Jacobs AR, Lanczycki CJ, Liebert CA, Liu C, Madej T, Marchler-Bauer A, Marchler GH, Mazumder R, Nikolskaya AN, Rao BS, Panchenko AR, Shoemaker BA, Simonyan V, Song JS, Thiessen PA, Vasudevan S, Wang Y, Yamashita RA, Yin JJ, Bryant SH. MMDB: Entrez's 3D-structure database. Nucleic Acids Res. 2003; 31:474–477. [PubMed: 12520055]

Cottrell GT, Burt JM. Functional consequences of heterogeneous gap junction channel formation and its influence in health and disease. Biochim Biophys Acta. 2005; 1711:126–141. [PubMed: 15955298]

Das Sarma J, Wang F, Koval M. Targeted gap junction protein constructs reveal connexin-specific differences in oligomerization. J Biol Chem. 2002; 277:20911–20918. [PubMed: 11929864]

Das S, Smith TD, Das Sarma J, Ritzenthaler JD, Maza J, Kaplan BE, Cunningham LA, Suaud L, Hubbard MJ, Rubenstein RC, Koval M. ERp29 restricts connexin43 oligomerization in the endoplasmic reticulum. Mol Biol Cell. 2009; 20:2593–2604. [PubMed: 19321666]

Das Sarma J, Das S, Koval M. Regulation of connexin43 oligomerization is saturable. Cell Commun Adhes. 2005; 12:237–247. [PubMed: 16531319]

Das Sarma J, Kaplan BE, Willemsen D, Koval M. Identification of rab20 as a potential regulator of connexin43 trafficking. Cell Commun Adhes. 2008; 15:65–74. [PubMed: 18649179]

Daugherty BL, Ward C, Smith T, Ritzenthaler JD, Koval M. Regulation of heterotypic claudin compatibility. J Biol Chem. 2007; 282:30005–30013. [PubMed: 17699514]

Figueroa XF, Isakson BE, Duling BR. Connexins: gaps in our knowledge of vascular function. Physiology (Bethesda). 2004; 19:277–284. [PubMed: 15381756]

Gabriels JE, Paul DL. Connexin43 is highly localized to sites of disturbed flow in rat aortic endothelium but connexin37 and connexin40 are more uniformly distributed. Circ Res. 1998; 83:636–643. [PubMed: 9742059]

Gemel J, Valiunas V, Brink PR, Beyer EC. Connexin43 and connexin26 form gap junctions, but not heteromeric channels in co-expressing cells. J Cell Sci. 2004; 117:2469–2480. [PubMed: 15128867]

Gong X, Agopian K, Kumar NM, Gilula NB. Genetic factors influence cataract formation in α3 connexin knockout mice. Dev Genet. 1999; 24:27–32. [PubMed: 10079508]

Heberlein KR, Straub AC, Isakson BE. The myoendothelial junction: breaking through the matrix? Microcirculation. 2009; 16:307–322. [PubMed: 19330678]

Hirst-Jensen BJ, Sahoo P, Kieken F, Delmar M, Sorgen PL. Characterization of the pH-dependent interaction between the gap junction protein connexin43 carboxyl terminus and cytoplasmic loop domains. J Biol Chem. 2007; 282:5801–5813. [PubMed: 17178730]

Hoehenwarter W, Tang Y, Ackermann R, Pleissner KP, Schmid M, Stein R, Zimny-Arndt U, Kumar NM, Jungblut PR. Identification of proteins that modify cataract of mouse eye lens. Proteomics. 2008; 8:5011–5024. [PubMed: 19003866]

Isakson BE, Duling BR. Heterocellular contact at the myoendothelial junction influences gap junction organization. Circ Res. 2005; 97:44–51. [PubMed: 15961721]

Isakson BE, Best AK, Duling BR. Incidence of protein on actin bridges between endothelium and smooth muscle in arterioles demonstrates heterogeneous connexin expression and phosphorylation. Am J Physiol Heart Circ Physiol. 2008; 294:H2898–H2904. [PubMed: 18408134]

Johnson R, Hammer M, Sheridan J, Revel JP. Gap junction formation between reaggregated Novikoff hepatoma cells. Proc Natl Acad Sci USA. 1974; 71:4536–4540. [PubMed: 4373716]

Johnson RG, Reynhout JK, Tenbroek EM, Quade BJ, Yasumura T, Davidson KG, Sheridan JD, Rash JE. Gap junction assembly: roles for the formation plaque and regulation by the C-terminus of connexin43. Mol Biol Cell. 2012; 23:71–86. [PubMed: 22049024]

Johnstone S, Isakson B, Locke D. Biological and biophysical properties of vascular connexin channels. Int Rev Cell Mol Biol. 2009; 278:69–118. [PubMed: 19815177]

Kanter HL, Saffitz JE, Beyer EC. Molecular cloning of two human cardiac gap junction proteins, connexin40 and connexin45. J Mol Cell Cardiol. 1994; 26:861–868. [PubMed: 7966354]

Koval M. Pathways and control of connexin oligomerization. Trends Cell Biol. 2006; 16:159–166. [PubMed: 16490353]

Koval M, Geist ST, Westphale EM, Kemendy AE, Civitelli R, Beyer EC, Steinberg TH. Transfected connexin45 alters gap junction permeability in cells expressing endogenous connexin43. J Cell Biol. 1995; 130:987–995. [PubMed: 7642714]

Koval M, Harley JE, Hick E, Steinberg TH. Connexin46 is retained as monomers in a *trans*-Golgi compartment of osteoblastic cells. J Cell Biol. 1997; 137:847–857. [PubMed: 9151687]

Lagree V, Brunschwig K, Lopez P, Gilula NB, Richard G, Falk MM. Specific amino-acid residues in the N-terminus and TM3 implicated in channel function and oligomerization compatibility of connexin43. J Cell Sci. 2003; 116:3189–3201. [PubMed: 12829738]

Laird DW. Life cycle of connexins in health and disease. Biochem J. 2006; 394:527–543. [PubMed: 16492141]

Laird DW. The gap junction proteome and its relationship to disease. Trends Cell Biol. 2010; 20:92–101. [PubMed: 19944606]

Maeda S, Nakagawa S, Suga M, Yamashita E, Oshima A, Fujiyoshi Y, Tsukihara T. Structure of the connexin 26 gap junction channel at 3.5 Å resolution. Nature. 2009; 458:597–602. [PubMed: 19340074]

Martínez AD, Maripillán J, Acuña R, Minogue PJ, Berthoud VM, Beyer EC. Different domains are critical for oligomerization compatibility of different connexins. Biochem J. 2011; 436:35–43. [PubMed: 21348854]

Maza J, Mateescu M, Sarma JD, Koval M. Differential oligomerization of endoplasmic reticulum-retained connexin43/connexin32 chimeras. Cell Commun Adhes. 2003; 10:319–322. [PubMed: 14681035]

Maza J, Das Sarma J, Koval M. Defining a minimal motif required to prevent connexin oligomerization in the endoplasmic reticulum. J Biol Chem. 2005; 280:21115–21121. [PubMed: 15817491]

Minogue PJ, Liu X, Ebihara L, Beyer EC, Berthoud VM. An aberrant sequence in a connexin46 mutant underlies congenital cataracts. J Biol Chem. 2005; 280:40788–40795. [PubMed: 16204255]

Musil LS, Goodenough DA. Multisubunit assembly of an integral plasma membrane channel protein, gap junction connexin43, occurs after exit from the ER. Cell. 1993; 74:1065–1077. [PubMed: 7691412]

Paznekas WA, Karczeski B, Vermeer S, Lowry RB, Delatycki M, Laurence F, Koivisto PA, Van Maldergem L, Boyadjiev SA, Bodurtha JN, Jabs EW. *GJA1* mutations, variants, and connexin 43 dysfunction as it relates to the oculodentodigital dysplasia phenotype. Hum Mutat. 2009; 30:724–733. [PubMed: 19338053]

Reed KE, Westphale EM, Larson DM, Wang HZ, Veenstra RD, Beyer EC. Molecular cloning and functional expression of human connexin37, an endothelial cell gap junction protein. J Clin Invest. 1993; 91:997–1004. [PubMed: 7680674]

Severs NJ, Rothery S, Dupont E, Coppen SR, Yeh HI, Ko YS, Matsushita T, Kaba R, Halliday D. Immunocytochemical analysis of connexin expression in the healthy and diseased cardiovascular system. Microsc Res Tech. 2001; 52:301–322. [PubMed: 11180622]

Wang Y, Addess KJ, Chen J, Geer LY, He J, He S, Lu S, Madej T, Marchler-Bauer A, Thiessen PA, Zhang N, Bryant SH. MMDB: annotating protein sequences with Entrez's 3D-structure database. Nucleic Acids Res. 2007; 35:D298–D300. [PubMed: 17135201]

Wittig I, Braun HP, Schagger H. Blue native PAGE. Nat Protoc. 2006; 1:418–428. [PubMed: 17406264]

Yeh HI, Rothery S, Dupont E, Coppen SR, Severs NJ. Individual gap junction plaques contain multiple connexins in arterial endothelium. Circ Res. 1998; 83:1248–1263. [PubMed: 9851942]

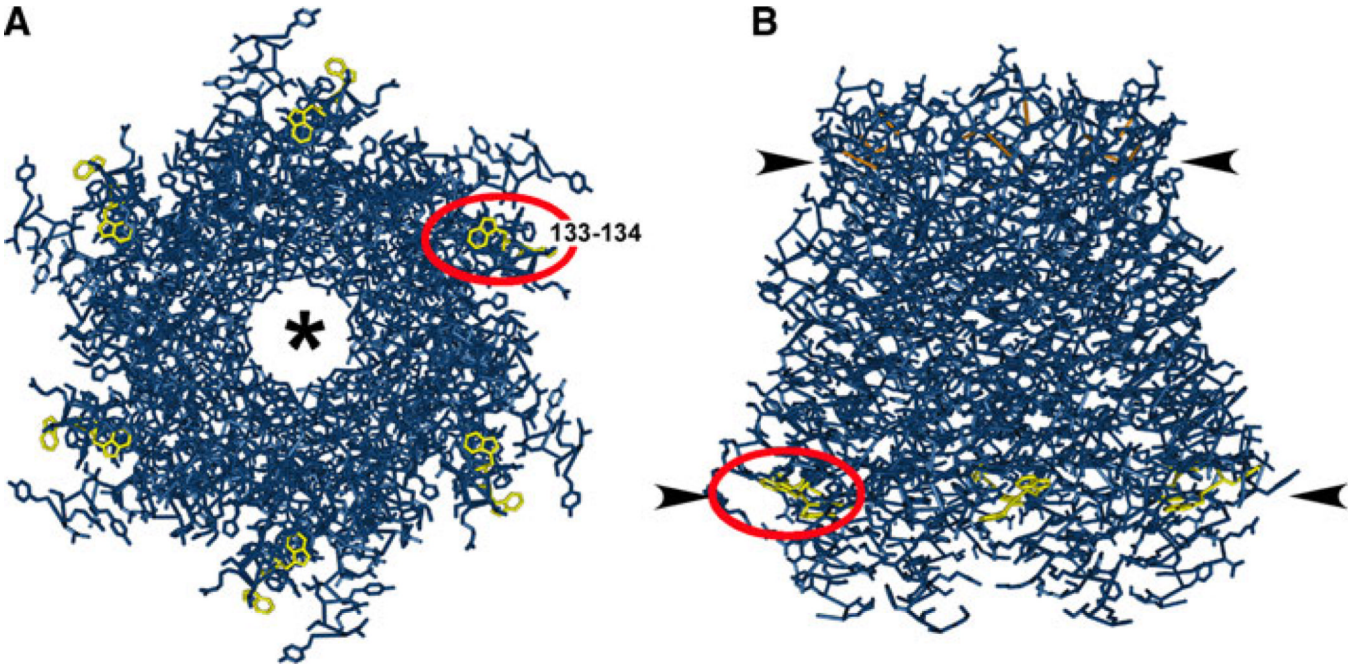

Fig. 1.

Localization of the Cx26 ditryptophan (WW) motif to the cytoplasmic membrane–aqueous interface based on the structural model. A tube-style structural model of Cx26 including side chains (Maeda et al. 2009) was produced using the Molecular Modeling Database (Wang et al. 2007; Chen et al. 2003). The WW motif at amino acids 133–134 (*red oval*) is highlighted in *yellow*. Disulfide bonds in the EL domains are highlighted in *orange*. **a** View from the cytosolic aspect of a Cx26 hemichannel looking up through the aqueous pore (*). **b** Side view of a Cx26 hemichannel in a membrane bilayer. Positions of the membrane–aqueous interfaces are denoted by *arrowheads*. Note that the WW motif is located at the membrane interface of the cytoplasmic leaflet

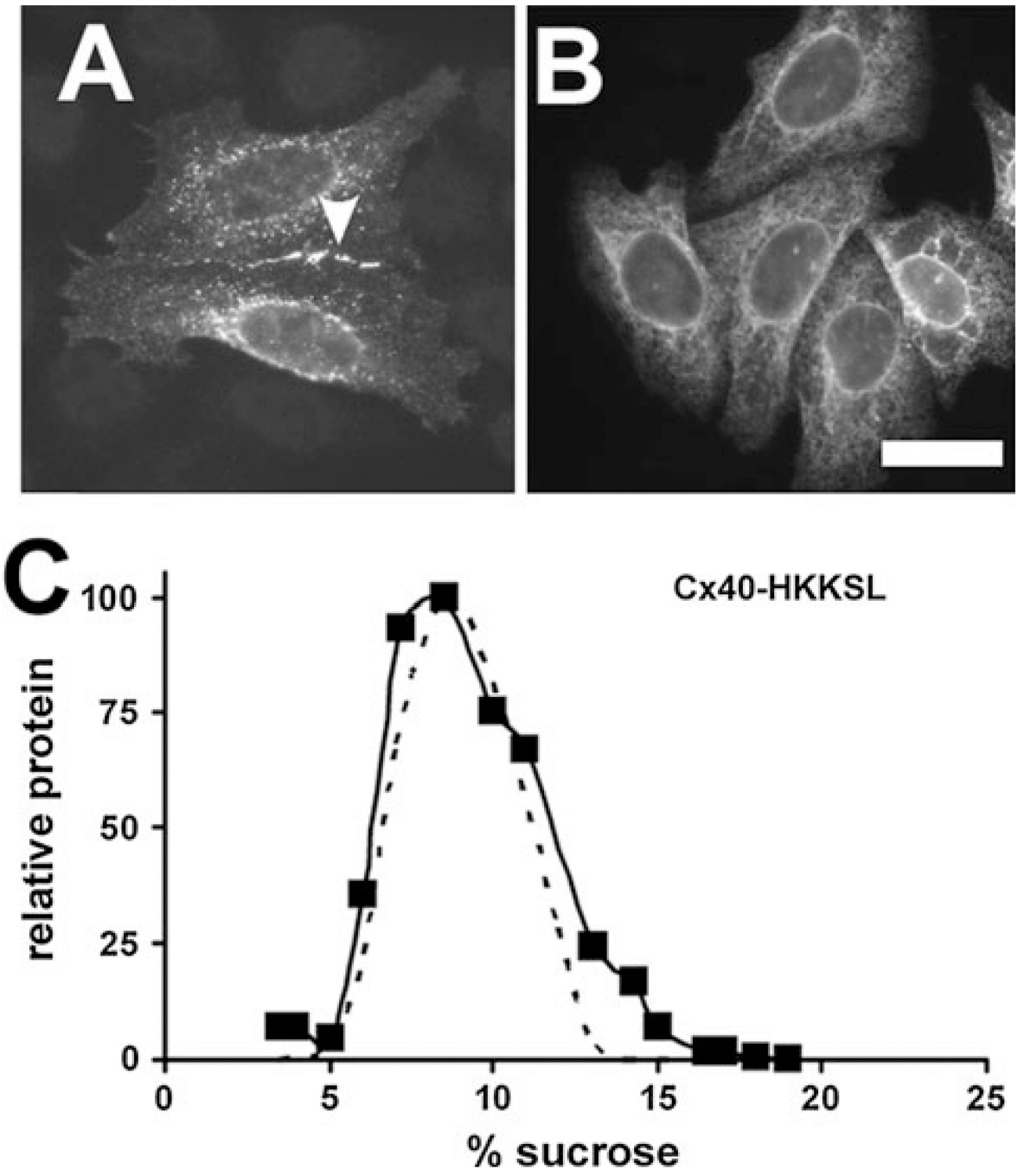

Fig. 2.

ER-retained Cx40 is monomeric. **a, b** HeLa cells transfected with either Cx40 (**a**) or Cx40-HKKSL (**b**) were fixed and immunostained. Untagged Cx40 was transported to the plasma membrane, where it formed gap junction plaques (*arrowhead*). By contrast, Cx40-HKKSL was retained in the ER. **c** HeLa/Cx40-HKKSL cells (*squares*) or HeLa/Cx43-HKKSL cells (*dashed line*) were processed and analyzed by sucrose gradient fractionation. Cx40-HKKSL had a similar profile on the gradient as Cx43-HKKSL, indicating that the ER-resident pool was monomeric. *Bar* 10 μm

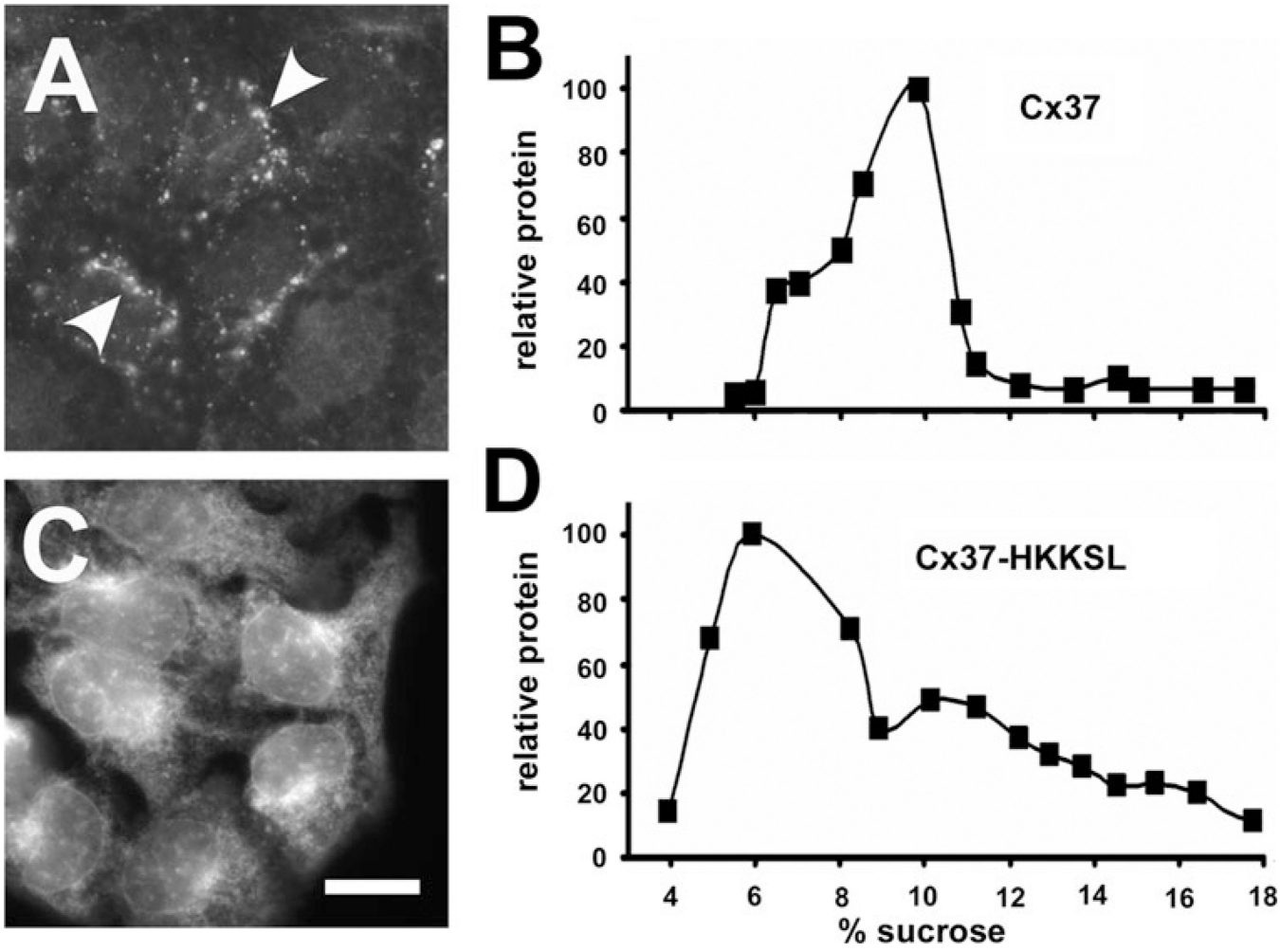

Fig. 3.

ER-retained Cx37 is partially oligomerized. **a, c** HeLa cells transfected with either Cx37 (**a**) or Cx37-HKKSL (**c**) were fixed and immunostained. Untagged Cx37 was transported to the plasma membrane, where it formed gap junction plaques (*arrowheads*). By contrast, Cx37-HKKSL was retained in the ER. *Bar* 10 μm. **b, d** HeLa/Cx37 (**b**) and HeLa/Cx37-HKKSL (**d**) cells were processed and analyzed by sucrose gradient fractionation. About one-third of Cx37-HKKSL migrated as oligomers at a peak centered at 10 % sucrose that comigrated with the predominant peak of untagged Cx37

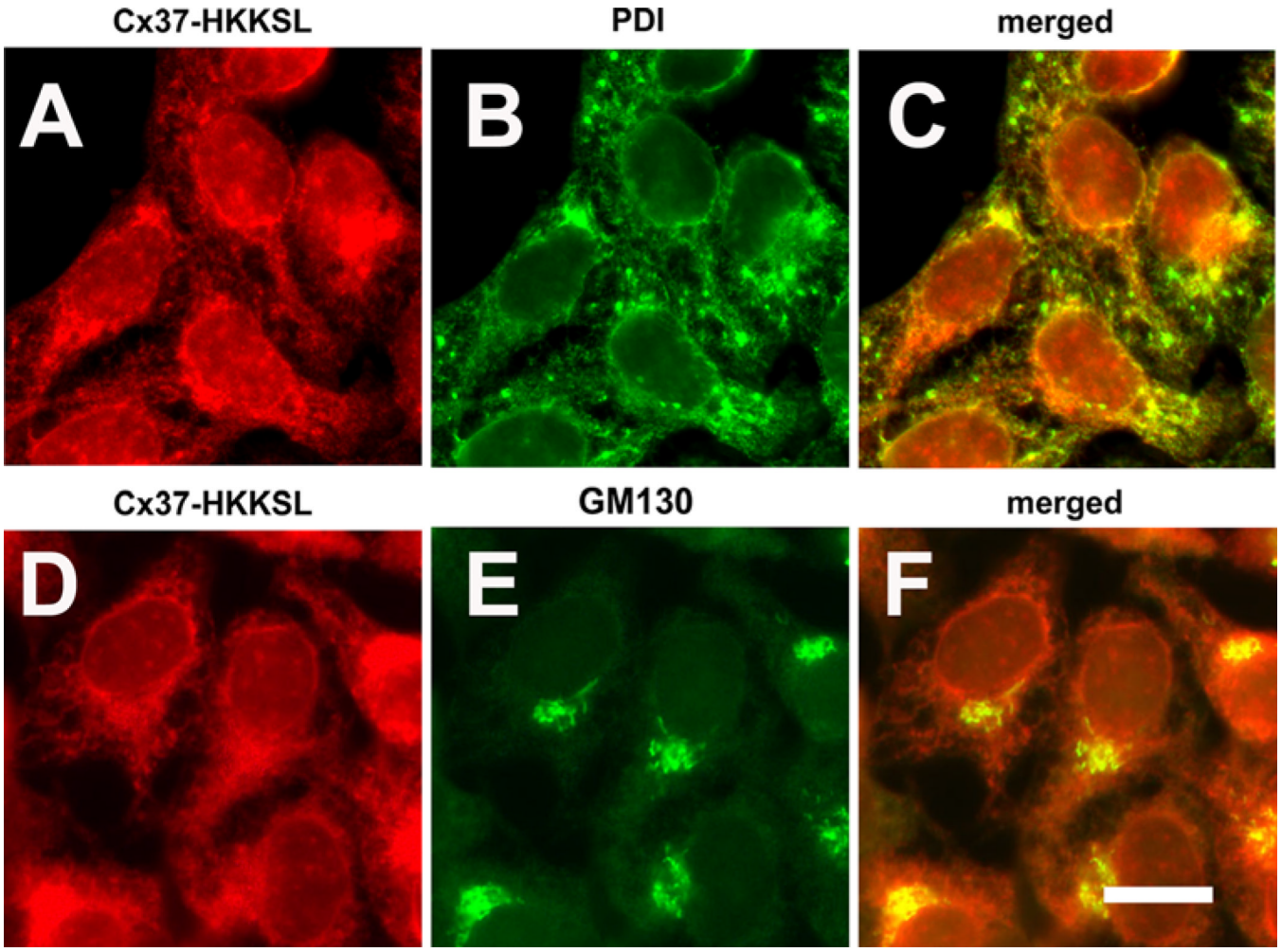

Fig. 4.

Cx37-HKKSL localized to the ER and Golgi apparatus. HeLa cells transfected with Cx37-HKKSL were fixed, permeabilized and then immunolabeled for Cx37 (**a, d**; *red*) and an ER marker, protein sulfide isomerase (PDI) (**b**, *green*) or a marker for the *cis* Golgi apparatus (GM130) (**e**, *green*). Merged images are shown in (**c, f**). Most Cx37-HKKSL colocalized with PDI, consistent with ER localization. A small fraction of Cx37-HKKSL colocalized with GM130, suggesting low levels of transport to the *cis* aspect of the Golgi apparatus. *Bar* 10 μm

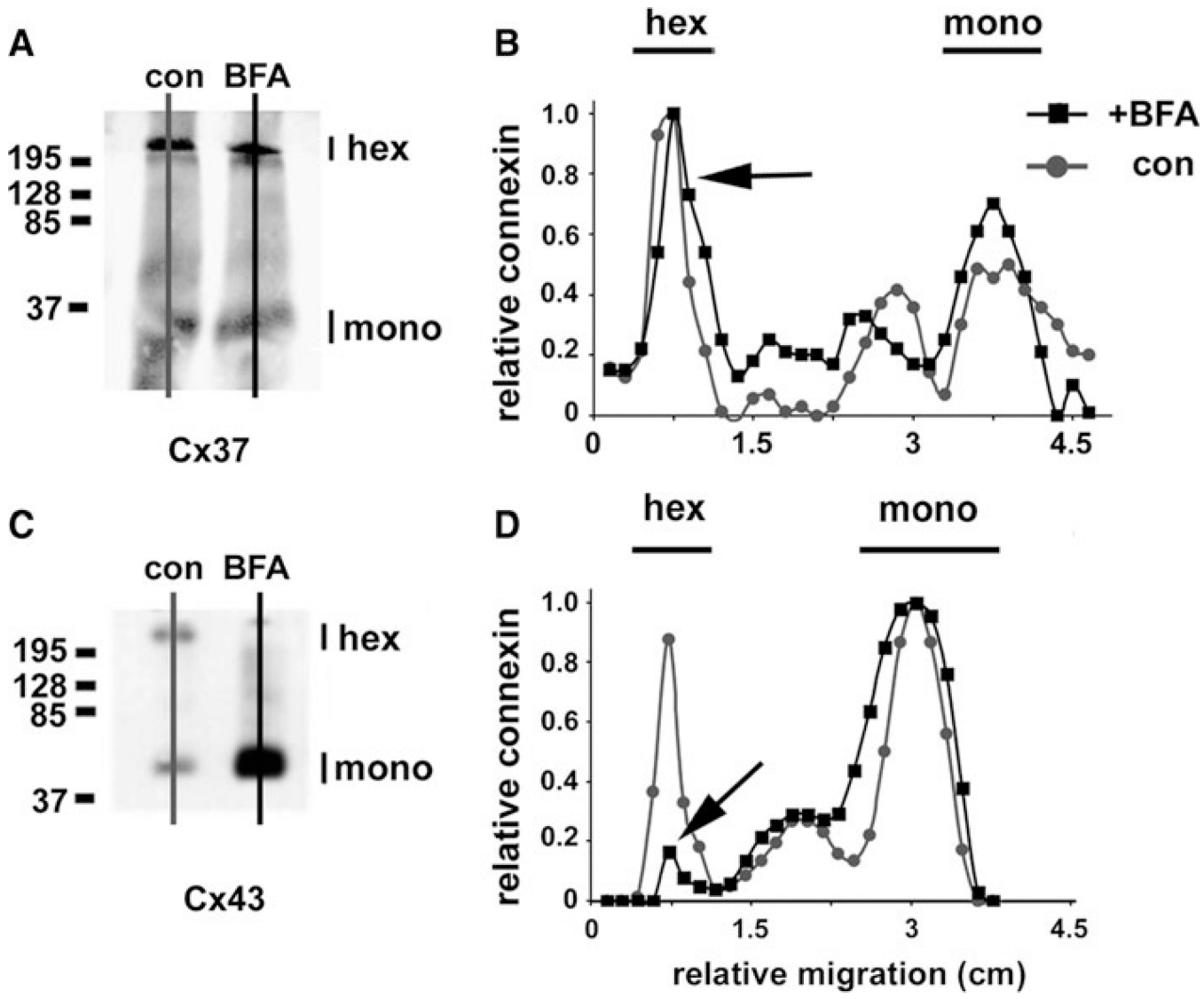

Fig. 5.

Cx37 oligomerization is insensitive to brefeldin A. HeLa cells transfected with either Cx37 (**a, b**) or Cx43 (**c, d**) were incubated in either the presence (*squares*) or the absence (*circles*) of 6 μg/ml brefeldin A (*BFA*) for 5 h, then harvested and solubilized in 0.1 % Triton X-100. Proteins were resolved by blue native gel electrophoresis and then transferred to Immobilon membranes. Cx37 and Cx43 were visualized by immunoblot. The Cx43 hexamer peak was considerably reduced by BFA treatment (**d**, *arrow*). In contrast to Cx43, the electrophoretic migration pattern for native Cx37 was not affected by BFA. Comparable levels of hexamers were detected in the presence and absence of the drug (**b**, *arrow*)

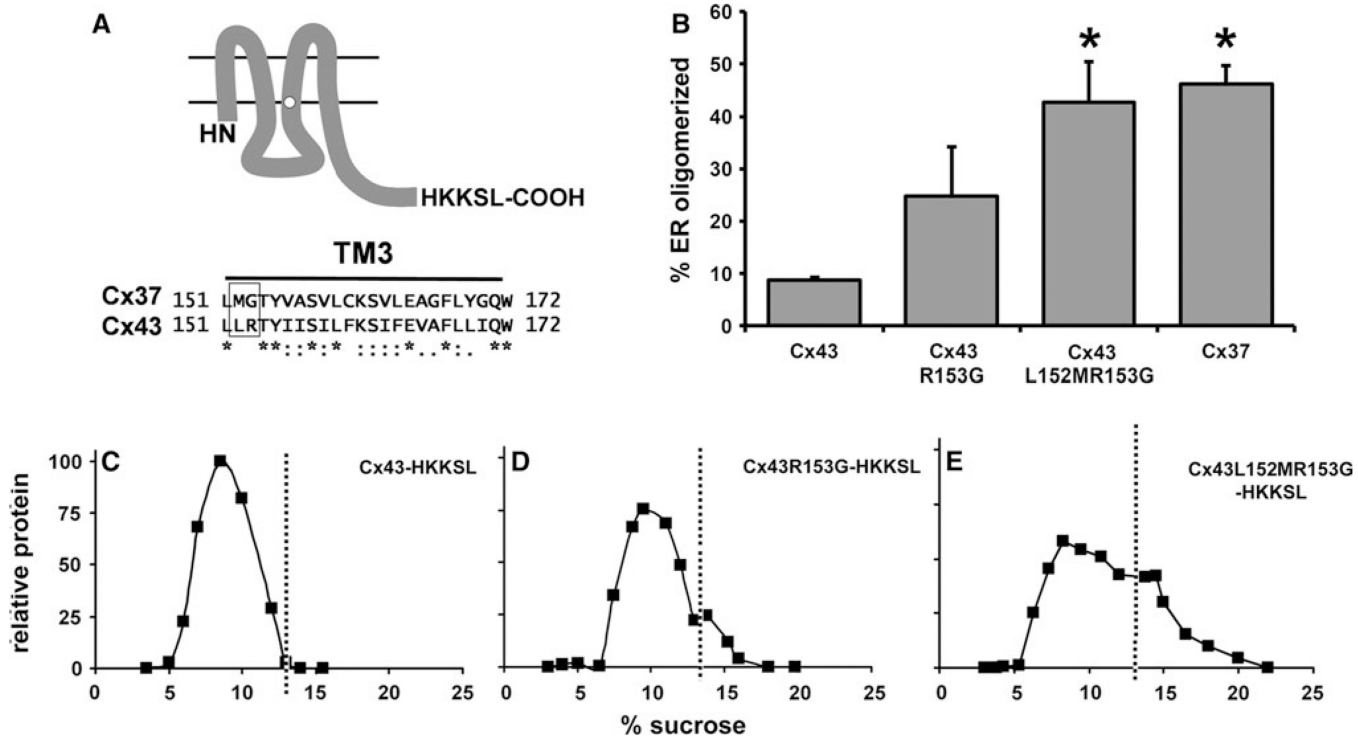

Fig. 6.

Mutating the cytoplasmic membrane interface region of the Cx43 TM3 from LR to MG destabilizes ER-retained monomers. **a** *Top* Diagram showing the plasma membrane topology of a connexin monomer (with an HKKSL tag appended to its C terminus). *Bottom* Sequence alignment of the TM3 domains of Cx37 and Cx43 shows the cytoplasmic interface motif surrounded by a *box*. **b** *Graph* shows the percentage of ER oligomerization calculated from profiles of sucrose gradient fractionation of HeLa cells transfected with Cx43-HKKSL, Cx43R153G-HKKSL, Cx43L152MR153G-HKKSL or Cx37-HKKSL (average ± SE, $n = 3$). The sucrose gradient profiles of Cx43L152-MR153G-HKKSL and Cx37-HKKSL were comparable and contained significantly more oligomerized connexins than Cx43-HKKSL (*$p < 0.01$). **c–e** Representative sucrose gradient profiles are shown for HeLa cells transfected with Cx43-HKKSL (**c**), Cx43R153G-HKKSL (**d**) or Cx43L152MR153G-HKKSL (**e**) dashed lines indicate the upper limit of the monomer peak in the gradient profiles (A representative sucrose gradient fractionation profile for Cx37-HKKSL is shown in Fig. 3)

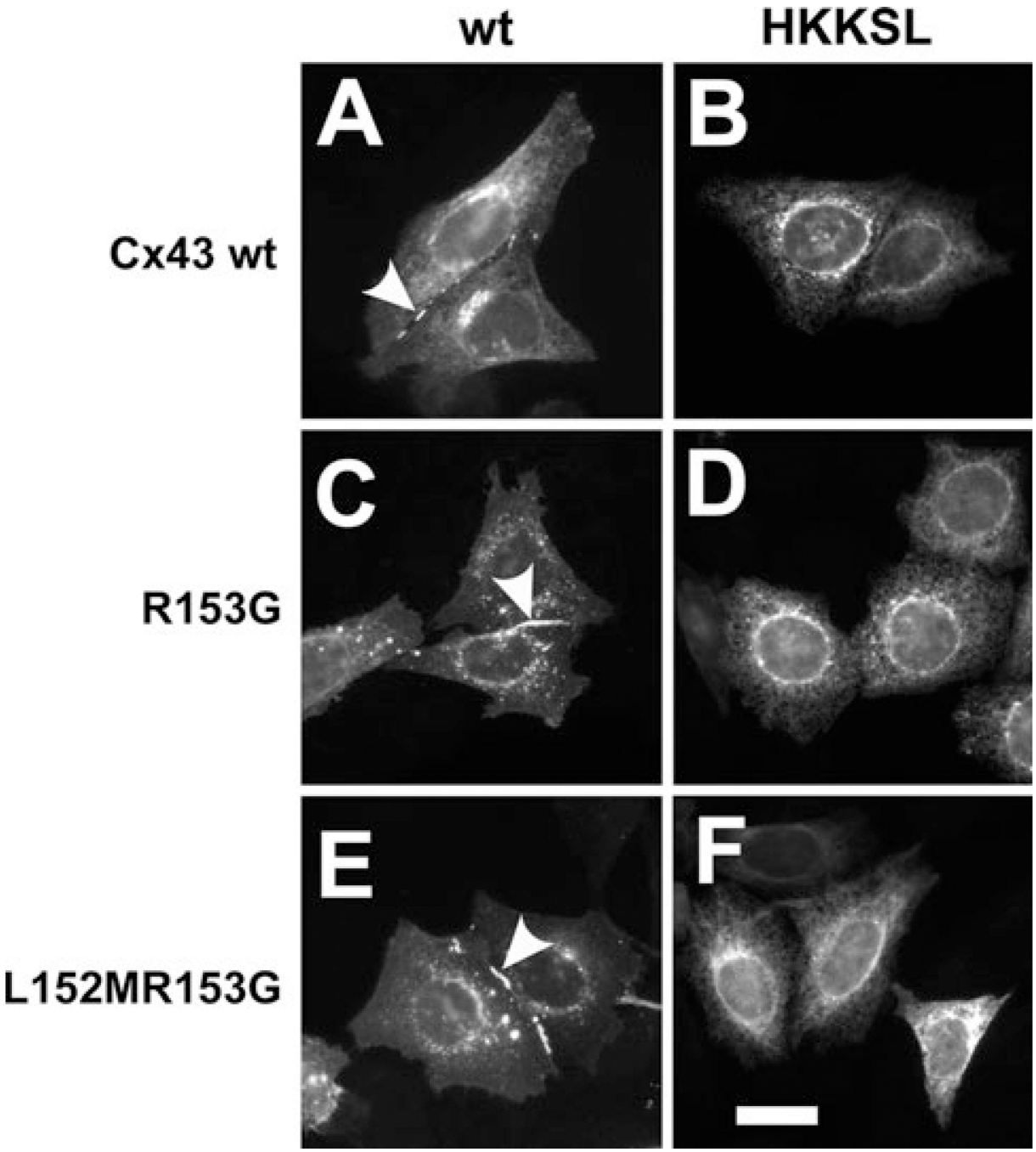

Fig. 7.

Cx43 mutants at the cytoplasmic membrane interface region of TM3 lacking the ER retention signal form gap junction plaques. HeLa cells transfected with Cx43 (**a**), Cx43-HKKSL (**b**), Cx43R153G (**c**), Cx43R153G-HKKSL (**d**), Cx43L152MR153G (**e**) or Cx43L152-MR153G-HKKSL (**f**) were fixed, permeabilized and then immunolabeled for Cx43. All untagged constructs formed gap junction plaques (*arrowheads*), indicating that they were properly folded and transported to the plasma membrane (**a, c, e**). By contrast, the HKKSL-tagged constructs showed ER localization (**b, d, f**). *Bar* 10 μm

Table 1

Connexin motifs in the cytoplasmic membrane interface region of TM3

Connexin		Amino acids	Motif
R type			
Cx43	GJA1	151–155	LLRTY
Cx46	GJA3	145–149	LLRTY
Cx50	GJA8	147–151	LLRTY
Cx62	GJA10	153–157	LLRTY
Cx45	GJC1	173–177	LMKIY
Cx47	GJC2	209–213	LMRVY
Cx36	GJD2	195–199	ISRFY
Cx31.9	GJD3	132–136	ARRCY
W type			
Cx32	GJB1	131–135	LWWTY
Cx26	GJB2	132–136	LWWTY
Cx31	GJB3	127–131	LWWTY
Cx30.3	GJB4	127–131	LWWTY
Cx31.1	GJB5	127–131	LWWTY
Cx30	GJB6	132–136	LWWTY
Cx25	GJB7	120–124	LWYAY
Cx30.2	GJC3	133–137	LLWAY
Other			
Cx37	GJA4	151–155	LMGTY
Cx40	GJA5	149–153	LLNTY
Cx59	GJA9	153–157	LLCTY
Cx40.1	GJD4	139–143	FSAGY
Cx23	GJE1	112–116	YTIIY